Regiospecific Synthesis and Structural Studies of 3,5-Dihydro-4 H -pyrido[2,3- b][1,4]diazepin-4-ones and Comparison with 1,3-Dihydro-2 H -benzo[b][1,4]diazepin-2-ones

David Nunez Alonso, Marta Perez-Torralba, Rosa M. Claramunt, Carmen Torralba, Patricia Delgado-Martinez, Ibon Alkorta, José Elguero, Christian Roussel

HAL Id: hal-03178458
https://hal.science/hal-03178458

Submitted on 23 Mar 2021

Article

Regiospecific Synthesis and Structural Studies of 3,5-Dihydro-4H-pyrido[2,3-b][1,4]diazepin-4-ones and Comparison with 1,3-Dihydro-2H-benzo[b][1,4]diazepin-2-ones

David Núñez Alonso, Marta Pérez-Torralba,* Rosa M. Claramunt, M. Carmen Torralba, Patricia Delgado-Martínez, Ibon Alkorta, José Elguero, and Christian Roussel

Read Online

ACCESS | Metrics & More | Article Recommendations | SI Supporting Information

ABSTRACT: Nine 3,5-dihydro-4H-pyrido[2,3-b][1,4]diazepin-4-ones (**17**−**25**), some of which contain fluoro-substituents, have been regiospecifically prepared by reaction of 2,3-diaminopyridines with ethyl aroylacetates. In two cases, open intermediates have been isolated and these are related to the reaction pathway. The X-ray crystal structure of 1-methyl-4-phenyl-3,5-dihydro-4H-pyrido[2,3-b][1,4]-diazepin-4-one (**23**) has been solved (formula, $C_{15}H_{13}N_3O$; crystal system, monoclinic; space group, $C2/c$). This is an asymmetric unit constituted by a single nonplanar molecule and its conformational enantiomer due to the presence of the seven-membered diazepin-2-one moiety, which introduces a certain degree of torsion in the adjacent pyridine ring. The ^1H, ^{13}C, ^{15}N, and ^{19}F NMR spectra were obtained and the chemical shifts, together with those of the previously published 1,3-dihydro-2H-benzo[b][1,4]diazepin-2-ones (**1**−**16**), i.e., a total of 544 values, were successfully compared with the chemical shifts calculated at the gauge invariant atomic orbital (GIAO)/Becke, three-parameter, Lee−Yang−Parr (B3LYP)/6-311++G(d,p) level. The seven-membered ring inversion barrier in 5-benzyl-2-phenyl-3,5-dihydro-4H-pyrido[2,3-b][1,4]diazepin-4-one (**25**) was determined and, in conjunction with the data from the literature, compared with the B3LYP/6-311++G(d,p) computed values. This allowed the determination of several structural effects. The rotation about the exocyclic N1−CR bond was also calculated and its dynamic properties were discussed.

Pyrido[2,3-b][1,4]diazepin-4-ones   Benzo[b][1,4]diazepin-2-ones

■ INTRODUCTION

Benzo[b][1,4]diazepin-2-ones are much less important in medicinal chemistry than benzo[e][1,4]-diazepin-2-ones such as diazepam and, for this reason, they have been less studied. However, there are some important drugs that contain the benzo[b][1,4] structure, for instance, the anxiolytic clobazam (7-chloro-1-methyl-5-phenyl-1,5-benzodiazepine-2,4-dione)[1] and the atypical antipsychotic olanzapine ({2-methyl-4-(4-methyl-1-piperazinyl)-10H-thieno[2,3-b][1,5]-benzodiazepine}).[2] Note that there are compounds like nevirapine that are both [b] and [e] [1,4]diazepines.[3,4] We have previously published some results in the field of benzo[b][1,4]diazepines (Figure 1).[5−7]
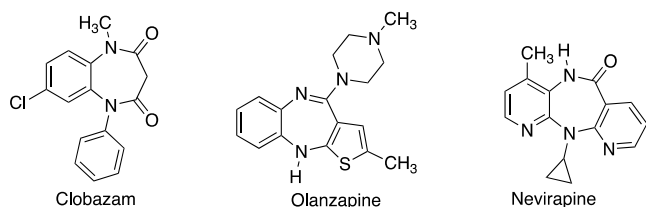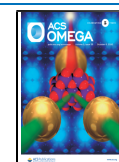
Several papers on benzo[b][1,4]diazepines have been published and these encompass new synthetic methodologies[8−10] and reactivity studies, including a comprehensive review[11] and a more recent reference.[12] The biological properties of benzo[b][1,4]diazepinones closely related to our work have been reported and the compounds are potent noncompetitive metabotropic glutamate receptor antagonists.[13] Finally, the ESIPT (excited-state intramolecular proton transfer) mechanism has been observed in the photochemistry of benzo[b][1,4]diazepinones.[14]

The biological importance of these compounds contrasts with the paucity of their structural studies. In this work, we present the regiospecific synthesis, X-ray crystallography data, and NMR (static and dynamic) properties of nine pyrido[2,3-b][1,4]-diazepin-4-ones, together with NMR data from our previous work concerning a series of sixteen benzo[b][1,4]diazepin-2-ones. Moreover, theoretical calculations of absolute shieldings

Figure 1. Structures of some benzo[b][1,4]diazepinones.

Clobazam   Olanzapine   Nevirapine

Figure 2. Benzo[*b*][1,4]benzodiazepin-2-ones and pyrido[2,3-*b*][1,4]diazepin-4-ones **1–25**.

Scheme 1. Substrate Scope for Substituted 2,3-Diaminopyridines

17 R_1=H, R_2=H, 61%[b]
18 R_1=H, R_2=F, 54%[b]
19 R_1=CH₃, R_2=H, 28%[b]
20 R_1=Cl, R_2=H, 25%[b]
21 R_1=Cl, R_2=Br, 36%[b]
22 R_1=CH₃, R_2=Br, 35%[b,c]

26 R_1=H, R_2=H
27 R_1=CH₃, R_2=Br

23 R_1=H, R_2=H, R= CH₃, 85%[b]
24 R_1=H, R_2=F, R= CH₃, 82%[b]
25 R_1=H, R_2=H, R= C₆H₅CH₂, 80%[b]

[a]120 °C, 24 h reaction time.
[b]Yields in isolated compound after purification.
[c]150 °C, 48 h reaction time.

(σ, ppm) and their transformation into chemical shifts (δ, ppm) have been carried out at the GIAO/B3LYP/6-311++G(d,p)

level to assign all NMR active nuclei (^{1}H, ^{13}C, ^{15}N, and ^{19}F) and enable the structures to be unambiguously identified. Moreover,

related theoretical calculations have been carried out to determine the inversion barriers of the diazepinone seven-membered ring in the gas phase.

■ RESULTS AND DISCUSSION

The structures of the compounds under study are depicted in Figure 2. Pyrido[2,3-b][1,4]diazepin-4-ones **17** to **25** have been synthesized for the first time in this work, and compounds **1−16** were described in our previous publications or elsewhere, a citation being provided in the corresponding tables.

Regiospecific Synthesis and Structural Studies of 3,5-Dihydro-4H-pyrido[2,3-b][1,4]diazepin-4-ones. The standard procedure to obtain 1,3-dihydro-2H-benzo[b][1,4]-diazepin-2-ones involves a condensation reaction in xylene at 120 °C between benzene-1,2-diamines and β-oxoesters, ethyl acetate, or ethyl aroylacetates. This method was used for the preparation of the N-unsubstituted 1,3-dihydro-4H-pyrido[2,3-b][1,4]diazepin-4-ones **17−22** starting from 2,3-diaminopyridines; in all cases, only one regioisomer was formed (Scheme 1). Open intermediates resulting from the condensation of the pyridine 2-amino group with the ester counterpart were isolated in two cases, **26** and **27**, as detailed in Experimental Section. Compounds **23−25** were obtained by subsequent N-alkylation under basic conditions.[15]

Our results differ from those of Israel et al.,[16,17] who described the formation of two regioisomers **I** and **II** in the reaction of 2,3-diaminopyridine with ethyl acetate. However, the results are consistent with those of Barchet and Merz[18] on the reaction of 2,3-diaminopyridine and ethyl benzoylacetate to yield compound **17**, albeit without any supporting structural data at that time (1964), and those of Israel on repeating the same reaction and establishing the structure of regioisomer **I** by thermal degradation of **17** to 1-(1-phenylvinyl)-1,3-dihydro-2H-imidazo[4,5-b]pyridin-2-one as a result of a [1,3] sigmatropic rearrangement (Scheme 2).[19]

Scheme 2. Regioisomers Formed in the Reaction of β-Oxoesters with 2,3-Diaminopyridine and Application of a Thermal Rearrangement Reaction to Establish Their Structure
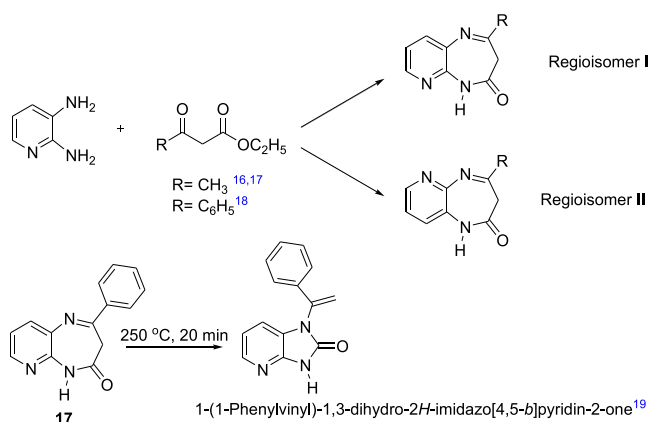
The synthesis of **17** was also described by Martins et al.[20] from the cyclocondensation reaction of 2,3-diaminopyridine with 1,1,1-trichloro-4-phenyl-4-methoxybut-3-en-2-one under basic conditions. The same group later isolated and characterized the open intermediate formed by addition of the 3-aminopyridine group to the β-olefinic carbon of the vinyl ketone, cyclization of which led to compound **17** (Scheme 3).[21]

Characterization and Imino/Enamino Tautomerism. Characterization of 3,5-dihydro-4H-pyrido[2,3-b][1,4]-diazepin-4-ones **17−25** was achieved by elemental analysis and multinuclear NMR spectroscopy. All classical 2D techniques, as well as spin−spin coupling constants, were used to assign the chemical shifts and these are consistent with the results of GIAO calculations (vide infra).

The ^{1}H, ^{13}C, ^{15}N, and ^{19}F NMR spectroscopic data in DMSO-d_6 or CDCl$_3$ solution (Table S1) confirmed that even if five tautomeric forms are possible (Scheme 4), they exist as the oxo-imino form **a** with, in some cases, small amounts of form **b**, as previously observed in compounds **1−16**.[6,7]

The presence of the oxo-enamino form **b** was detected in compounds **17** and **18** in proportions of 7 and 9%, respectively (Figure 3). The most relevant NMR features allowing the identification of both tautomeric forms are as follows: oxo-imino form **a**, δ of 3-CH$_2$ around 3.60 ppm, δ of 3-CH$_2$ at around 40 ppm; oxo-enamino form **b**, δ of 3-CH around 4.70 ppm, δ of 3-CH at around 96 ppm. Note that the atom numbering scheme used in Figure 3 differs from the IUPAC system but allows comparison between 1,3-dihydro-2H-benzo[b][1,4]diazepin-2-ones and 3,5-dihydro-4H-pyrido[2,3-b][1,4]diazepin-4-ones since, in both cases, the NH and NR nitrogen atom is N1 and the C═O group is on C2.

Note that the multiplicity of H3 in tautomer **b** differs between **17**, a triplet of ^4J = 2.2 Hz, and **18**, a doublet of ^4J = 2.3 Hz. The triplet corresponds to two identical coupling constants of 2.2 Hz between H3 and H1 and H5. The doublet of 2.3 Hz is probably due to the fact that, in **18**, one of the coupling constants is much smaller than the other, although an NH to ND proton exchange in DMSO-d_6 cannot be excluded.

Crystal Structure of Compound 23. Crystals of 5-methyl-2-phenyl-3,5-dihydro-4H-pyrido[2,3-b][1,4]diazepin-4-one (**23**) were grown from ethanol; the compound crystallizes in the C2/c space group belonging to the monoclinic system. The asymmetric unit is constituted by a single molecule that is not planar due to the presence of the seven-membered diazepin-2-one moiety, which introduces a certain degree of torsion in the adjacent pyridine ring. In this sense, the defined dihedral angle between the pyridine and phenyl rings is 49.8(2)° (Figure 4). The N1 atom is flat and the sum of the angles around it is 359.3°. Both M conformational enantiomers are present in the unit cell and these correspond to rotation about the C9A−N1 bond (−177.97° and +177.97° corresponding to M and P conformational enantiomers); the same angles calculated theoretically (gas phase) are ±174.9°.

However, a certain planarity is observed in the molecule in the pyridine-N1N5 fragment on the one hand and in the 4-phenyl-C3C4N5 unit on the other. The C2 carbonyl carbon points away from these two moieties and the distances to the aforementioned planes are 0.719(3) and 1.451(3) Å, respectively. This result, along with the electronic distribution observed, is consistent with the crystallographic angle and bond length data obtained for this compound, which corresponds to tautomer **a** with a C4═N5 double-bonded imino group. Molecules of **23** can be considered to be crystallographically isolated since there are no notable interactions between them, probably due to the presence of the methyl group on the N1 nitrogen atom, which prevents the formation of hydrogen bonds. The packing along the b axis is provided in Figure S1 (Supporting Information).

The structure obtained for pyrido[2,3-b][1,4]diazepin-4-one (**23**) has similar characteristics to those previously determined in benzo[b][1,4]diazepin-2-ones,[6,7] but less distortion is

Scheme 3. Martins' Reaction of 2,3-Diaminopyridine with Methoxyvinylketones
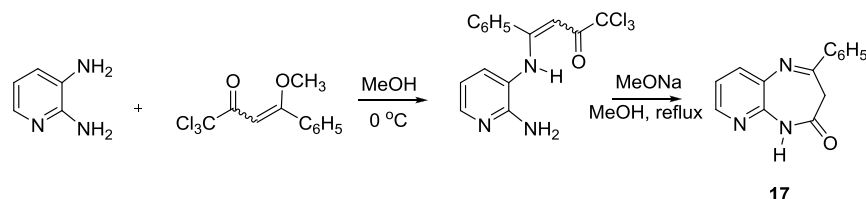
Scheme 4. Five Tautomeric Forms of 3,5-Dihydro-4*H*-pyrido[2,3-*b*][1,4]diazepin-4-ones
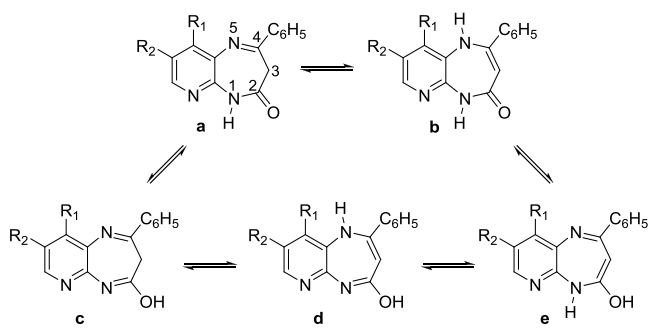
observed in the latter, where the dihedral angle between the benzo and phenyl rings lies in the range of $4.6(1)-25.8(1)°$ depending on the substituents, cf. a value of $49.8(2)°$ observed for **23** (Figure 5).

Comparison of Experimental and Calculated NMR Chemical Shifts. The experimental and calculated chemical shifts of compounds **1** to **25** (two calculated rotamers of the benzyl group of **25**) are gathered in Table S1 of the Supporting Information. The chemical shifts and coupling constants of compounds **17**−**25** are provided in Experimental Section.

The data for all the nuclei (^{1}H, ^{13}C, ^{15}N, and ^{19}F) in all the reported solvents (CDCl$_3$, DMSO-d_6, acetone-d_6, and THF-d_8) were analyzed using simple and multiple regressions. The resulting 544 values are represented in Figure 6. The fitted equation is

$$\text{experimental(ppm)} = (0.999 \pm 0.001)\text{calculated(ppm)}, \; n$$
$$= 544, \; R^2 = 0.9993, \; \text{RMS residual} = 2.7 \text{ ppm} \quad (1)$$

An examination of the residuals shows some systematic deviations. The compounds that present these deviations have NH protons and C−Br and C−Cl carbons. On introducing them as dummy variables (1, presence; 0, absence), the following multivariate equation was obtained

$$\text{experimental(ppm)} = (0.9998 \pm 0.0009)\text{calculated}$$
$$+ (3.7 \pm 0.6)\text{NH} - (18.2 \pm 1.6)\text{C} - \text{Br}$$
$$- (9.9 \pm 1.1)\text{C} - \text{Cl}, \; n = 544,$$
$$R^2 = 1.000, \; \text{RMS residual} = 2.3 \text{ ppm} \quad (2)$$

The new coefficients show that the ^{1}H NMR signal of the NH is shifted in different solvents by +3.7 ppm (on average for the four solvents) and that the C atoms bearing a Br or, to a lesser extent, a Cl atom, are not well calculated by GIAO because of relativistic effects, a well-known fact that we and others have already reported.[22−25]

Inversion Barriers of the Seven-Membered Rings. An interesting phenomenon was observed in compounds **23**−**25**

and this concerns the appearance of the two enantiotopic protons, endo (H3A)/exo (H3B) (see Figure 4) or axial and equatorial, Hax and Heq, or of the methylene group at position 3 in tautomer **a** at room (300 K) and low temperatures. These signals were used to determine the inversion barrier of 5-benzyl-2-phenyl-3,5-dihydro-4*H*-pyrido[2,3-*b*][1,4]diazepin-4-one (**25**) by recording the ^{1}H NMR spectra in THF-d_8 at different temperatures (Figure 7). The difference in the chemical shifts of the methylene protons depends on the structure of the compound and on the temperature; for instance, this signal is not observed in compounds **17** and **18** at room temperature.

The inversion process of the seven-membered ring of [1,4]diazepinones is similar to that of cycloheptatriene (inversion barrier, 26 kJ·mol^{-1})[26] and 7*H*-benzo[7]annulene. We determined the barrier for compound **25** (see Figure 7 and experimental part) and added other barriers from the literature and from our previous works (Table 1).

Table 1 is completed by calculating compounds **28** to **33** (Figure 8), for which experimental values are not available. Derivatives **28** to **32** were selected to cover complementary situations not found in the studied compounds, and quaternary salt **33** contributes to the discussion of the barriers.

Our goal is not to achieve precision but proportionality as the barriers often contain significant errors and various solvents have been used. An attempt to differentiate the solvents indicated that dimethyl sulfoxide and tetrahydrofuran increase the barrier by around 5 kJ·mol^{-1} with respect to chloroform, acetone, and toluene. In the discussion, solvent effects will not be considered. With the data of Table 1, different models were considered, giving rise to eqs 3−5 (units in kJ·mol^{-1}, Se = standard error)
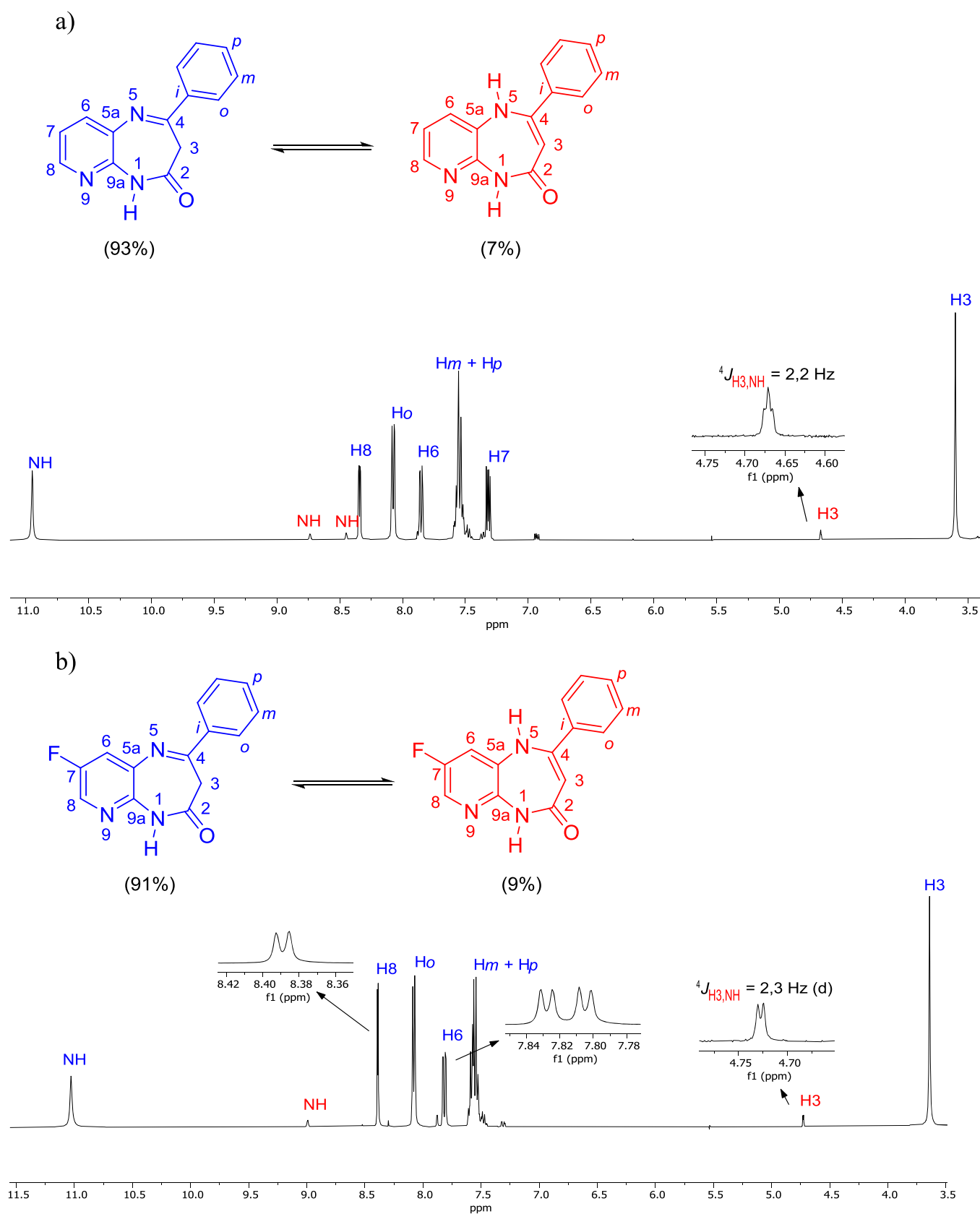
$$\text{exp.} = (7.1 \pm 6.2) + (1.06 \pm 0.11)\text{calc.}, \; n = 13, \; R^2$$
$$= 0.900, \; \text{Se} = 2.3 \quad (3)$$

$$\text{exp.} = (3.3 \pm 3.3) + (0.95 \pm 0.05)\text{calc.}$$
$$+ (8.8 \pm 1.9)\text{tetraF}, \; n = 13, \; R^2 = 0.970, \; \text{Se} = 2.8 \quad (4)$$

$$\text{exp.} = (1.00 \pm 0.02)\text{calc.} + (9.8 \pm 1.6)\text{tetraF}, \; n = 13, \; R^2$$
$$= 0.998, \; \text{Se} = 2.8 \quad (5)$$

The most important conclusion is that a correction term was necessary for 6,7,8,9-tetrafluoro-substituted compounds, i.e., **9**−**16** and **32**. Therefore, eq 4 was used to calculate the fitted and predicted values in Table 1. Since the intercept of eq 4 is not significant, it was imposed to be 0 to give eq 5.

In the case of compounds **23** and **24**, the proton signals of the methylene group at position 3 in DMSO-d_6 are lost in the baseline, meaning that the coalescence occurs at around 300 K; however, the signals can be observed in CDCl$_3$ at 300 K (Figure 9). The fitted values reported in Table 1 (52.8 and 53.6 kJ·mol^{-1}) are related to the experimental Δv values (see Figure 9 and Table S1, 400.13 and 468.15 Hz, respectively) through the

a)

b)

Figure 3. ^{1}H NMR spectra of (a) 2-phenyl-3,5-dihydro-4H-pyrido[2,3-b][1,4]diazepin-4-one (**17**) and (b) 8-fluoro-2-phenyl-3,5-dihydro-4H-pyrido[2,3-b][1,4]diazepin-4-one (**18**). The atom numbering is shown in the structures.

Eyring equation; the corresponding coalescence temperatures should be 301 K for **23** and 305 K for **24**, i.e., not far from 300 K

(Figure 7) but indicating that the predicted values are underestimated by eq 4.
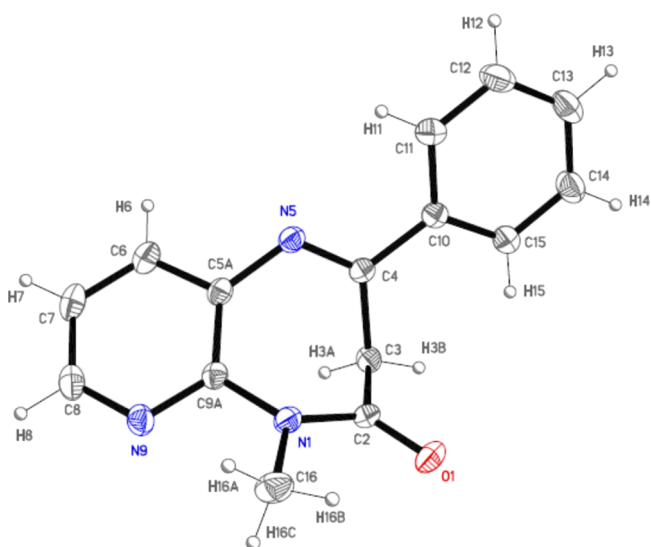
Figure 4. ORTEP plot (20% probability) of compound **23** showing the labeling of the corresponding asymmetric unit. The N bearing the methyl group is numbered N1.

Pyrido[2,3-*b*][1,4]diazepin-4-one (**23**)   Benzo[*b*][1,4]diazepin-2-one (**13**)

Figure 5. Comparative views of the molecular distortion in **23** and **13**.

The data in Table 1 (fitted and predicted) were used to calculate the differences related to the structures of compounds (see Figure S2 of the Supporting Information) and these are provided in Table 2. There are six main primary effects: replacing N_1H by N_1Me and then replacing N_1Me by N_1Bn, replacing C_2=O by C_2=S, replacing C_4-Me by C_4-Ph, replacing $CH_{6,7,8,9}$ by $CF_{6,7,8,9}$, and replacing C_9H by N_9. These primary effects are discussed assuming that they are independent, even if we are aware that, in empirical modeling,

this is an approximation,[29,30] because the action of secondary and even tertiary effects is apparent from the extreme values for some effects, e.g., −18.5/−43.7 for NH to NMe, +4.4/−11.6 for CO to CS, and +5.4/+13.9 for C_9H to N_9.

The calculations were performed on the CH_2 tautomer and the calculated barriers to inversion quantitatively associate a barrier in $kJ\cdot mol^{-1}$ to a single combination of R, X, Y, and R′ (Figure 10), covering a wide range of values. Qualitatively, the interconversion barrier arises from rotation around the $C_{9a}-N_1$ axis through a quasi-planar transition state (TS) in which R is facing Y, with the cyclic structure imposing some special features during the rotation. For instance, the C_2=X bond is pointing outward throughout the whole rotation process and, thus, the well-documented large change in the steric requirement upon going from C_2=O to C_2=S is not operating.[31] Replacing C_2=O by C_2=S increases the barrier by 5.5 $kJ\cdot mol^{-1}$ and the origin of that weak change is due to the stiffening of the N_1-C_2 bond upon going from amide to thioamide. The stiffening of the N_1-C_2 bond peaks in salt **33** (Figure 8) yields a barrier of 84.3 $kJ\cdot mol^{-1}$.

As one would expect, a large increase of the barrier (28.1 $kJ\cdot mol^{-1}$) is observed upon going from R = H to R = Me. A further increase of the barrier (6.5 $kJ\cdot mol^{-1}$) occurs upon going from R = Me to R = Bn. These changes result from the frontal interaction between Y = CH and R in the TS.

In the case of the 9-aza derivatives (Y = N), for R = H, the decrease of the barrier is 11.5 $kJ\cdot mol^{-1}$ on average. For N_1 = H (**3/17** pair), the effect is +5.4 $kJ\cdot mol^{-1}$; for N_1 = Me (**4/23** pair), the effect is +12.4 $kJ\cdot mol^{-1}$; and for N_1 = Bn (**5/25** pair), the effect is +13.2 $kJ\cdot mol^{-1}$. These results seem reasonable, bearing in mind the lower steric demand of the N atom and the possibility of forming HBs with the CH of Me and Bn groups. The lower steric demand and the H-bonding ability of Y = N is not the only contribution to the decrease of the barrier as the electron-attracting character of pyridine is prone to stabilizing of the almost planar transition state through cross-conjugation of the (thio)amide nitrogen atom.

A similar cross-conjugation is possibly at work when four desaturating F atoms were introduced on the aromatic part and this more than compensates for the small but significant steric effect of the fluorine atom in position 9.[32,33] The introduction of
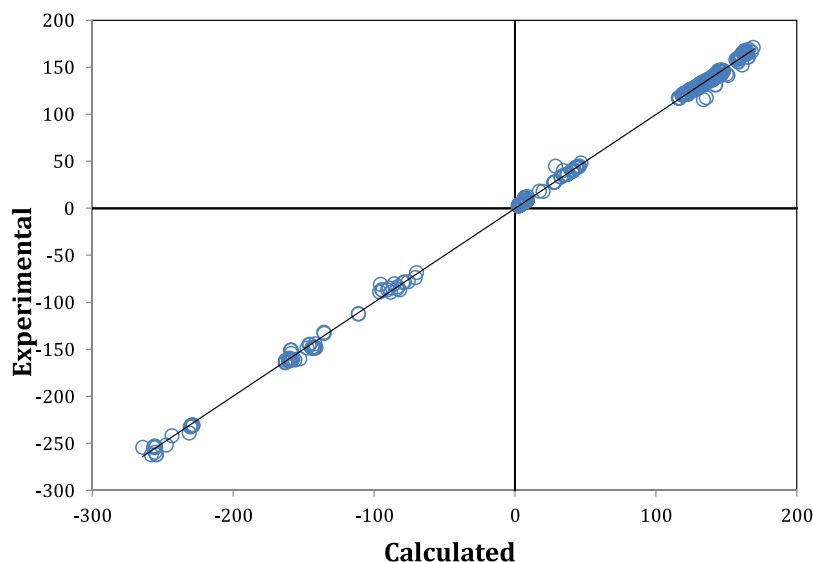
Figure 6. Plot of experimental versus calculated chemical shifts (ppm) for compounds **1** to **25**.
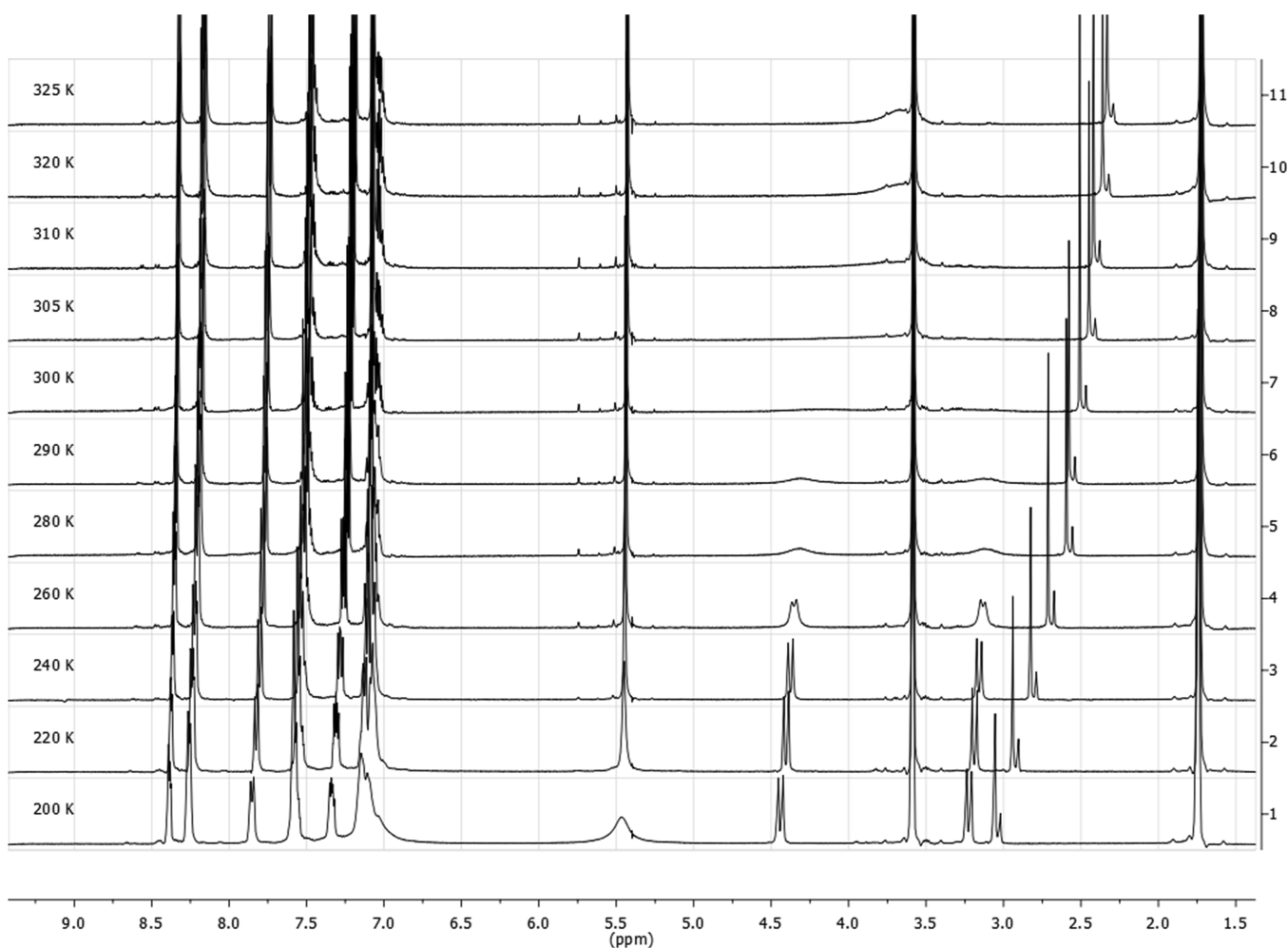
Figure 7. ^{1}H NMR spectra (in particular, the methylene protons of the two CH$_2$ groups) of compound **25** in THF-d_8 at different temperatures (200−325 K).

four F atoms increases the barrier by 18.3 kJ·mol^{-1} (or by 7.9 kJ·mol^{-1}, excluding compounds **14** and **32**) (Table 2). One must consider the electron-attracting effects of the pyridine nitrogen and the perfluoro substitution, which may stabilize the planar TS and thus contribute to the lowering of the barrier.[34,35]

A more complete approach that would include all interaction terms (primary, secondary, and tertiary) is possible and this involves the use of complete factorial designs. We will discuss only the case of compound **14** because **32** is a perturbation of **14** with increasing effects, which has a third-order interaction involving three terms NMe/tetraF/4Ph. The corresponding 2^3 matrix is provided in Table 3.

The resulting equation is as follows

$$\Delta G = a_0 + a_1 \text{NMe} + a_2 \text{tetraF} + a_3 \text{4Ph}$$
$$+ a_{12} \text{NMe/tetraF} + a_{13} \text{NMe/4Ph}$$
$$+ a_{23} \text{tetraF/4Ph} + a_{123} \text{NMe/tetraF/4Ph} \quad (6)$$

where the reference compound is **1**.

Since the matrix has eight independent variables and eight dependent ones, the correlation coefficient is 1. The results of the multiregression are as follows: $a_0 = 43.7$ (compound **1**); $a_1 = 20.4$; $a_2 = 0.0$; $a_3 = -4.0$; $a_{12} = 7.6$; $a_{13} = 5.1$; $a_{23} = 8.1$; $a_{123} = 10.6$.

The primary interactions are 20.4 (NMe), 0.0 (tetraF), and −4.0 kJ·mol^{-1} (4Ph) in which, when compared with the results of Table 2, 25.9, 7.9, and 1.7 kJ·mol^{-1}, respectively (excluding **14** and **32**), they are different, although the order is the same (shifted by 6−8 kJ·mol^{-1}). This finding stresses the danger of neglecting interaction terms.

Of the secondary interactions, it should be noted that NMe and tetraF on the one hand and 4Ph and tetraF on the other are in proximity, but NMe and 4Ph appear to be more remote. One possible explanation for this result is that the a_{13} interaction is transmitted through the four F atoms (Figure 11). Finally, it is worth highlighting the high values of the tertiary effect, NMe/tetraF/4Ph, $a_{123} = 10.6$ kJ·mol^{-1}. The structures of the minimum and the TS of **14** are provided in Figure 12 to show the conformational changes that occur in the TS.

Rotational Barriers of the *N*-Benzyl Group of Compound 25. Note that the signals of the enantiotopic methylene protons of the *N*-benzyl group at 5.44 ppm (Figure 7) are only broadened at 220 K, but the coalescence should occur far below 200 K. On comparison of the appearance of the two methylene signals, it is reasonable to assume that the T_C for the benzyl CH$_2$ protons is about 170 K. The different behavior of these two methylene groups is related to the difference in the chemical shifts. According to the calculated values (Table S2), the difference for C(3)H$_2$ is 1.60 ppm (experimental, 1.23 ppm), while for the benzyl group, it is only 0.34 ppm.

Table 1. Experimental (tw = This Work, nm = Not Measured) and Calculated Barriers of Benzo- and Pyrido[1,4]diazepinones in kJ·mol^{-1} [d]

comp.	ref.	Solvent	T_C (K), CH$_2$ ring	exp.	calc.	fitted & predicted
1	6, 27	[a]	203	39.8	42.4	43.7[b]
2	6, 28	nm	nm		63.8	64.1[c]
3	6, 28	acetone	181	41.8	38.2	39.7[b]
4	6, 28	acetone	268.5	65.3	65.0	65.2[b]
5	6, 28	acetone	267	67.0	71.7	71.6[b]
6	28	acetone	206	46.9	41.9	43.2[b]
7	28	acetone	306	79.5	77.1	76.8[b]
8	28	DMSO-d_6	306	82.5	80.1	79.6[b]
9	6	toluene-d_8	230	42.6	42.4	43.7[b]
10	6	toluene-d_8	263	69.9	61.9	71.7[b]
11	7	THF-d_8	263	48.9	37.5	47.8[b]
12	7	THF-d_8	251	47.7	38.4	48.7[b]
13	7	THF-d_8	245	47.3	35.8	46.2[b]
14	7	DMSO-d_6	>373		83.3	91.5[c]
15	7	toluene-d_8	>373		79.7	88.0[c]
16	7	DMSO-d_6	>373		81.1	89.4[c]
17	tw	DMSO-d_6	300 K		32.5	34.3[c]
18	tw	DMSO-d_6	300 K		33.6	35.3[c]
19	tw	DMSO-d_6	300 K		37.0	38.6[c]
20	tw	DMSO-d_6	300 K		36.2	37.8[c]
21	tw	DMSO-d_6	300 K		37.7	39.2[c]
22	tw	DMSO-d_6	300 K		39.0	40.5[c]
23	tw	CDCl$_3$	300 K (broad)		51.9	52.8[c]
24	tw	CDCl$_3$	300 K (broad)		52.8	53.6[c]
25	tw	THF-d_8	303	56.6	57.8	58.4[b]
28	tw				28.9	30.9[c]
29	tw				49.2	50.2[c]
30	tw				37.8	39.3[c]
31	tw				75.6	75.3[c]
32	tw				95.0	102.6[c]
33	tw				85.0	84.3[c]

[a]Pyridine-d_5/CDCl$_3$. [b]Fitted. [c]Predicted. [d]Experimental values correspond to ΔG_{TC}. Fitted and predicted values from eq 2 are also reported.

Taddei *et al.*[28] discussed the possibility that the coalescence of the methylene ring signals was due to a N$_1$–R pyramidal inversion, but they rejected this proposal by analogy with results obtained with benzo[e][1,4]diazepin-2-ones. In fact, the N$_1$ atom is planar as in amides; for the three *N*-benzyl derivatives, the sum of the angles around N1 is 359.9° for compounds **5**, **8**, and **25**. Experimentally, the sum of these angles for the *N*-methyl compound **23** is 359.3° (Figure 4).

We calculated the rotation profile of the *N*-benzyl substituent of compound **25**. The dihedral is defined as C$_{ipso}$–C(H$_2$)–N1–C$_{9a}$ (Figure 13).
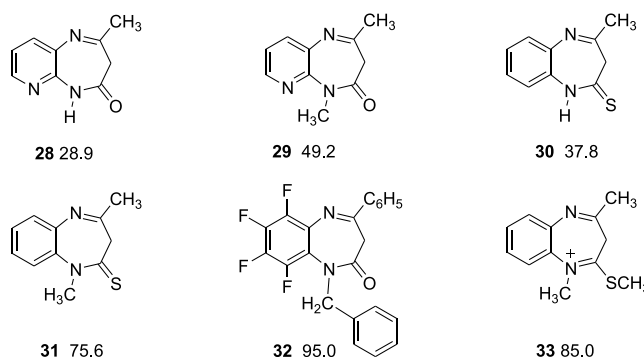
Figure 8. Calculated barriers in kJ·mol^{-1} for compounds **28** to **33** (compound **28** is the regioisomer **I**, R = Me, depicted in Scheme 2).

From 0° to 360°, there are two minima and two TSs: 1st TS, ϕ = 26.8°, E_{rel} = 32.7 kJ·mol^{-1}; 1st minimum, ϕ = 105.9°, E_{rel} = 6.1 kJ·mol^{-1}; 2nd TS, ϕ = 175.4°, E_{rel} = 35.8 kJ·mol^{-1}; 2nd minimum, ϕ = 281.8°, E_{rel} = 0.0 kJ·mol^{-1}. The TSs are much lower in energy than those of the ring inversion, which means that they do not contribute to the broadening of the signals. Furthermore, rotation cannot exchange the benzylic protons. As a consequence, the observed broadening of the benzyl methylene proton signals is due to the ring inversion (ΔG = 51,700 J·mol^{-1}) and the much lower T_C (170 K vs 303 K) to the marked decrease in $\Delta \nu$ (H$_A$/H$_B$ separation).

The difference in energy between the two rotamers is 6100 J·mol^{-1}, which corresponds to 92% of the most stable one at 303 K and to 98% of the most stable one at 170 K. It was decided to ascertain whether the differences in calculated chemical shifts (Table S1, mainly affecting signals of the *N*-benzyl group) compared with the experimental ones could be sufficient to determine the structure of the most stable conformer, i.e., the principal minimum vs secondary minimum. To this end, we carried out a statistical analysis of the data using simple regressions. The results are reported in Table 4.

The differences are not dramatic, but all of them point in the same direction, namely, the largest square correlation coefficient, slope closer to 1, and intercept closer to 0, thus indicating that the rotamer present in solution is indeed that of lower energy (1st minimum).

■ CONCLUSIONS

The main conclusions of this work are as follows:

1. Nine new 3,5-dihydro-4*H*-pyrido[2,3-*b*][1,4]diazepin-4-ones, **17** to **25**, have been prepared regiospecifically.

2. Two new examples of oxo-imino/oxo-enamino tautomerism have been reported in the family of pyrido[2,3-*b*][1,4]diazepin-4-ones.

3. A large series of experimental chemical shifts, 544 values, has been successfully correlated with those calculated at the GIAO/B3LYP/6-311++G(d,p) level and this allows the prediction of those values that were not determined.

4. The inversion barriers, measured or estimated, of the seven-membered ring have been compared with those calculated at the B3LYP/6-311++G(d,p) level. The total set has been successfully analyzed, taking into account several structure effects.

5. The effects on the inversion barriers have been discussed (a) considering the properties of atoms, bonds, and steric effects and (b) using a complete factorial design that includes primary, secondary, and tertiary effects. This

Compound **23** in CDCl₃ at 300 K   Compound **24** in CDCl₃ at 300 K
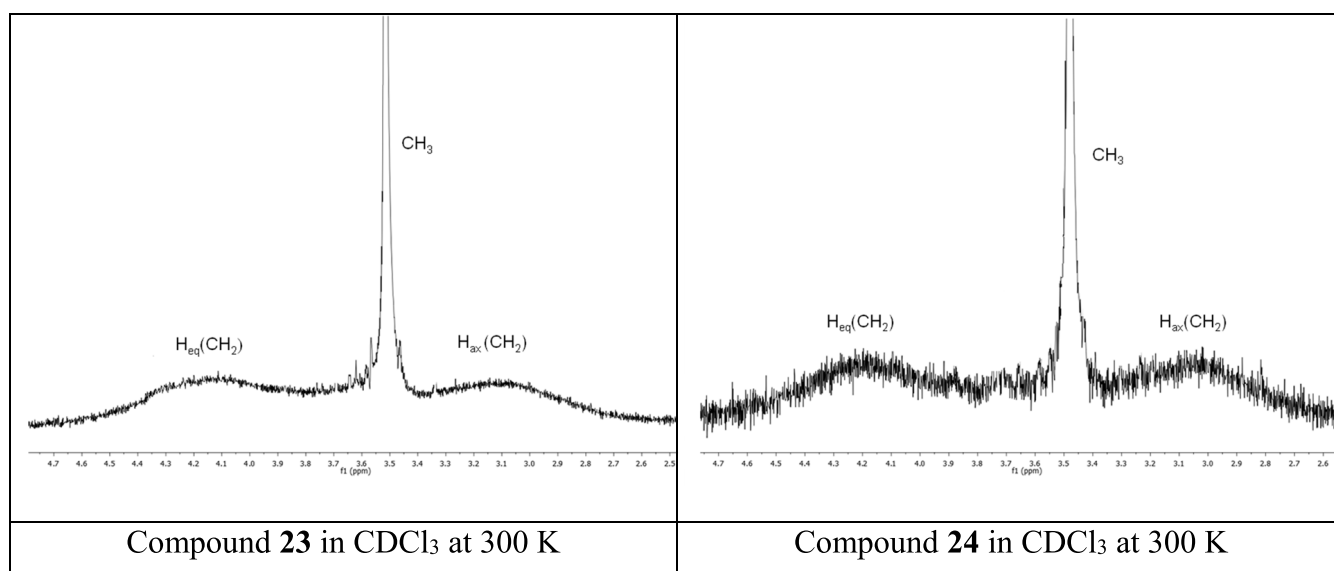
Figure 9. ^{1}H NMR spectra at 300 K of the methylene group at position 3 for compounds **23** and **24**.

model shows the importance of secondary and tertiary interactions that were not previously taken into account.

6. In the case of the *N*-benzyl derivative **25**, the rotation of the benzyl group has been calculated and discussed in relation to the experimental evidence.

■ EXPERIMENTAL SECTION

General Information. All chemicals used in the synthetic procedures were commercial compounds. Melting points were determined by DSC with a DSC 220 C instrument (SEIKO Instruments Inc., Torrance, CA, USA) connected to a model SSC5200H disk station. Thermograms (sample size, 0.003–0.005 g) were recorded at a scan rate of 5.0 °C. Column chromatography was performed on silica gel (Merck 60, 70–230 mesh) and elemental analyses were carried out on a LECO-CHNS-932 apparatus.

NMR Parameters and DNMR. Solution spectra were recorded on a 9.4 T spectrometer (400.13 MHz for ^{1}H, 379.50 MHz for ^{19}F, 100.62 MHz for ^{13}C, and 40.56 MHz for ^{15}N) at 300 K with a 5 mm inverse detection H-X probe equipped with a z-gradient coil or with a QNP 5 mm probe (19F). Chemical shifts (δ in ppm) are referred to the internal solvent: DMSO-d_6, 2.49 for ^{1}H and 39.5 for [13]C. External references were used for ^{15}N and ^{19}F, namely, nitromethane and CFCl₃, respectively. Signals were characterized as s (singlet), d (doublet), t (triplet), and m (multiplet).

2D experiments ([1]H-^{1}H) gs-NOESY, ([1]H-^{13}C) gs-HMQC, (^{1}H-^{13}C) gs-HMBC, ([1]H-^{15}N) gs-HMQC, (^{1}H-^{15}N) gs-HMBC, (^{19}F-^{19}F) gs-COSY, and ([1]H-^{19}F) gs-HOESY were carried out with the standard pulse sequences[36] to assign the ^{1}H, ^{13}C, ^{15}N, and ^{19}F signals. The numbering system used in the NMR assignments is provided in Figure 14.

Variable temperature spectroscopy was performed using a Bruker BVT3000 temperature unit to control the temperature of the cooling gas stream and an exchanger to achieve low temperatures. To avoid problems at low temperatures caused by air moisture, pure nitrogen was used as the bearing, driving, and cooling gas. The procedure for calculating the barrier of compound (**25**) is reported in Table S2 (Supporting Information).

Synthetic Procedures. Compounds **1−10**[6] and **11−16**[7] were prepared as previously described.

2-Phenyl-3,5-dihydro-4H-pyrido[2,3-b][1,4]diazepin-4-one (17). 2,3-Diaminopyridine (0.15 g, 1.39 mmol) and ethyl benzoylacetate (0.25 mL, 1.45 mmol) in anhydrous xylene (8 mL) were heated at 120 °C for 24 h. The mixture was cooled down and a solid precipitated. This residue was washed with ethyl ether to give compound **17** (0.20 g, 61%) as a pale yellow solid: mp 270.7 °C (EtOH), lit. mp 264−266 °C,[18] 258 °C,[19] 250−252 °C;[21] ^{1}H NMR (400.13 MHz, DMSO-d_6) δ 10.95 (s, 1H, H1), 8.34 (dd, $^3J_{H7}$ = 4.6, $^4J_{H6}$ = 1.8 Hz, 1H, H8), 8.08 (dd, $^3J_{Hm}$ = 7.7, $^4J_{Hp}$ = 1.2 Hz, 2H, Ho), 7.85 (dd, $^3J_{H7}$ = 7.9, $^4J_{H8}$ = 1.8 Hz, 1H, H6), 7.55 (m, 3H, Hm, Hp), 7.32 (dd, $^3J_{H6}$ = 7.9, $^3J_{H8}$ = 4.6 Hz, 1H, H7), 3.60 (s, 2H, H3); ^{13}C NMR (100.62 MHz, DMSO-d_6) δ 166.2 (C2), 159.4 (C4), 146.1 (C8), 142.5 (C9a), 136.9 (Ci), 136.5 (C6), 134.6 (C5a), 131.1 (Cp), 128.8 (Cm), 127.8 (Co), 120.1 (C7), 40.3 (C3); ^{15}N NMR (40.54 MHz, DMSO-d_6) δ −231.3 (N1), n.o. (N5), −84.8 (N9); anal. calcd for C₁₄H₁₁N₃O (237.26): C, 70.87; H, 4.67; N, 17.71. Found: C, 70.44; H, 4.59; N, 17.69.

8-Fluoro-2-phenyl-3,5-dihydro-4H-pyrido[2,3-b][1,4]-diazepin-4-one (18). 5-Fluoro-2,3-diamino-pyridine (0.50 g, 3.94 mmol) and ethyl benzoylacetate (0.71 mL, 4.07 mmol) in anhydrous xylene (8 mL) were heated at 120 °C for 24 h. The mixture was cooled down and a solid precipitated. The residue was washed with ethyl ether to give compound **18** (0.54 g, 54%) as a pale yellow solid: mp 267.2 °C (EtOH); ^{1}H NMR (400.13 MHz, DMSO-d_6) δ 11.03 (s, 1H, H1), 8.39 (d, $^4J_{H6}$ = 2.8 Hz, 1H, H8), 8.08 (dd, $^3J_{Hm}$ = 6.9, $^4J_{Hp}$ = 1.7 Hz, 2H, Ho), 7.82 (dd, $^3J_{F7}$ = 9.2, $^4J_{H8}$ = 2.8 Hz, 1H, H6), 7.55 (m, 3H, Hm, Hp), 3.64 (s, 2H, H3); ^{13}C NMR (100.62 MHz, DMSO-d_6) δ 165.4 (C2), 160.6 (C4), 155.2 (C7, $^1J_{F7}$ = 250.9), 138.9 (C9a), 136.4 (Ci), 134.9 (C5a, $^3J_{F7}$ = 7.3), 133.4 (C8, $^2J_{F7}$ = 25.2), 131.1 (Cp), 128.3 (Cm), 127.4 (Co), 121.6 (C6, $^2J_{F7}$ = 20.0), 40.1 (C3); ^{15}N NMR (40.54 MHz, DMSO-d_6) δ −232.6 (N1), n.o. (N5), −80.4 (N9); ^{19}F NMR (376.50 MHz, DMSO-d_6) δ −133.2 (d, $^3J_{H6}$ = 9.3 Hz, 1F, F7); anal. calcd for C₁₄H₁₀FN₃O (255.25): C, 65.88; H, 3.95; N, 16.46. Found: C, 65.56; H, 3.89; N, 16.46.

9-Methyl-2-phenyl-3,5-dihydro-4H-pyrido[2,3-b][1,4]-diazepin-4-one (19). 4-Methyl-2,3-diamino-pyridine (0.50 g,

Table 2. Differences Corresponding to Six Effects (in kJ·mol⁻¹)[a]
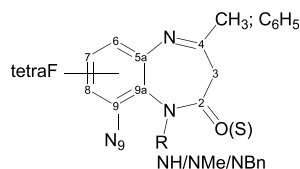
number of effects	effect	pair of compounds	$\Delta\Delta G$ (kJ·mol⁻¹)	mean value	difference	mean value excluding **14** and **32** (in italics)
8	N₁H to N₁Me	1 → 2	−20.4	−28.1	+7.7	−25.9
		3 → 4	−25.5		+2.6	
		6 → 7	−33.6		−5.5	
		9 → 10	−28.0		+0.1	
		17 → 23	−18.5		+9.6	
		28 → 29	−19.3		+8.8	
		30 → 31	−36.0		−7.9	
		11 → 14	−43.7		−15.6	
4	N₁Me to N₁Bn	4 → 5	−6.4	−6.5	+0.1	−4.9
		7 → 8	−2.8		+3.7	
		23 → 25	−5.6		+9.0	
		14 → 32	*−11.1*		*−4.6*	
4	C₂O to C₂S	1 → 30	+4.4	−5.5	−9.9	−5.5
		2 → 31	−11.2		−5.7	
		3 → 6	−3.5		+2.0	
		4 → 7	−11.6		−6.1	
7	4Me to 4Ph	1 → 3	+4.0	−4.3	+8.3	−1.7
		2 → 4	−1.1		+3.2	
		9 → 11	−4.1		+0.2	
		28 → 17	−3.4		+0.9	
		30 → 6	−4.0		+0.3	
		31 → 7	−1.5		+2.8	
		10 → 14	*−19.8*		*−15.5*	
4	tetrafluoro	2 → 10	−7.6	−18.3	+10.7	−7.9
		3 → 11	−8.1		+10.2	
		4 → 14	*−26.3*		*−8.0*	
		5 → 32	*−31.0*		*−12.7*	
5	C₉H to N₉	1 → 28	+12.8	+11.5	+1.3	+11.5
		2 → 29	+13.9		+2.4	
		3 → 17	+5.4		−6.1	
		4 → 23	+12.4		+0.9	
		5 → 25	+13.2		+1.7	

[a]$\Delta\Delta G$ values were calculated from the fitted and predicted ΔG values of Table 1.
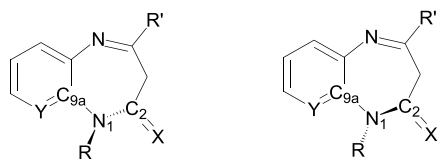

Figure 10. Conformational changes that occur in the seven-membered ring inversion.

4.06 mmol) and ethyl benzoylacetate (0.72 mL, 4.16 mmol) in anhydrous xylene (8 mL) were heated at 120 °C for 24 h. The mixture was cooled down and a solid precipitated. This residue was washed with ethyl ether to give compound **19** (0.29 g, 28%) as a pale yellow solid: mp 280.3 °C (EtOH); ¹H NMR (400.13 MHz, DMSO-d_6) δ 10.80 (s, 1H, H1), 8.20 (d, $^3J_{H7}$ = 4.7 Hz, 1H, H8), 8.11 (dd, $^3J_{Hm}$ = 7.6, $^4J_{Hp}$ = 2.0 Hz, 2H, Ho), 7.56 (m, 3H, Hm, Hp), 7.20 (d, $^3J_{H8}$ = 4.7 Hz, 1H, H7), 3.57 (s, 2H, H3), 2.44 (s, 3H, Me); ¹³C NMR (100.62 MHz, DMSO-d_6) δ 166.3 (C2), 157.9 (C4), 145.6 (C6), 145.4 (C8), 142.0 (C9a), 137.0 (Ci), 133.4 (C5a), 131.2 (Cp), 128.8 (Cm), 127.6 (Co), 121.5

(C7), 40.4 (C3), 17.8 (Me); ¹⁵N NMR (40.54 MHz, DMSO-d_6) δ −230.4 (N1), n.o. (N5), −81.0 (N9); anal. calcd for $C_{15}H_{13}N_3O$ (251.29): C, 71.70; H, 5.21; N, 16.72. Found: C, 71.16; H, 5.15; N, 16.60.

9-Chloro-2-phenyl-3,5-dihydro-4H-pyrido[2,3-b][1,4]-diazepin-4-one (20). 4-Chloro-2,3-diamino-pyridine (0.50 g, 3.48 mmol) and ethyl benzoylacetate (0.62 mL, 3.59 mmol) in anhydrous xylene (8 mL) were heated at 120 °C for 24 h. The mixture was cooled down and a solid precipitated. This residue was washed with ethyl ether to give compound **20** (0.24 g, 25%) as a pale yellow solid: mp 261.6 °C (EtOH); ¹H NMR (400.13 MHz, DMSO-d_6) δ 11.16 (s, 1H, H1), 8.29 (d, $^3J_{H7}$ = 5.1 Hz, 1H, H8), 8.12 (d, $^3J_{Hm}$ = 7.4 Hz, 2H, Ho), 7.57 (m, 3H, Hm, Hp), 7.51 (d, $^3J_{H8}$ = 5.1 Hz, 1H, H7), 3.69 (s, 2H, H3); ¹³C NMR (100.62 MHz, DMSO-d_6) δ 166.2 (C2), 160.3 (C4), 146.3 (C8), 143.7 (C9a), 141.1 (C6), 136.5 (Ci), 131.8 (Cp), 131.7 (C5a), 128.9 (Cm), 128.0 (Co), 120.9 (C7), 40.8 (C3); ¹⁵N NMR (40.54 MHz, DMSO-d_6) δ −230.4 (N1), n.o. (N5), −89.1 (N9); anal. calcd for $C_{14}H_{10}ClN_3O$ (271.70): C, 61.89; H, 3.71; N, 15.47. Found: C, 61.45; H, 3.72; N, 15.47.

Table 3. Matrix Corresponding to eq 6[a]

comp.	NMe, a_1	tetraF, a_2	4Ph, a_3	NMe/tetraF, a_{12}	NMe/4Ph, a_{13}	tetraF/4Ph, a_{23}	NMe/tetraF/4Ph, a_{123}	ΔG
1	0	0	0	0	0	0	0	43.7
2	1	0	0	0	0	0	0	64.1
3	0	0	1	0	0	0	0	39.7
4	1	0	1	0	1	0	0	65.2
9	0	1	0	0	0	0	0	43.7
10	1	1	0	1	0	0	0	71.7
11	0	1	1	0	0	1	0	47.8
14	1	1	1	1	1	1	1	91.5

[a]ΔG values are the fitted and predicted values from Table 1.
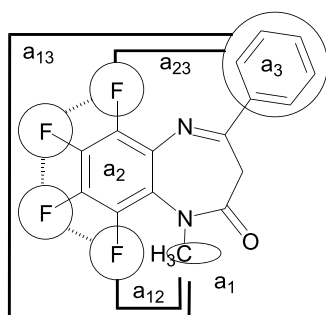
Figure 11. Primary and secondary interactions in compound **14**.
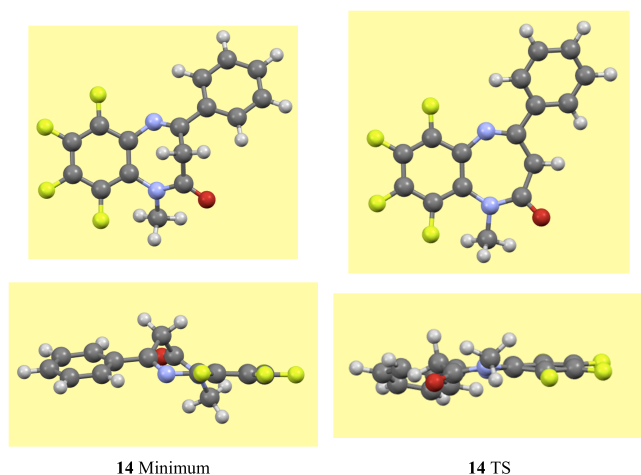

14 Minimum　　　　**14** TS

Figure 12. Two views of the minimum and TS of the inversion of the seven-membered ring of **14**.

8-Bromo-9-chloro-2-phenyl-3,5-dihydro-4H-pyrido[2,3-b][1,4]diazepin-4-one (21). 5-Bromo-4-chloro-2,3-diaminopyridine (0.50 g, 2.25 mmol) and ethyl benzoylacetate (0.40 mL, 2.32 mmol) in anhydrous xylene (8 mL) were heated at 120 °C for 24 h. Purified by column chromatography using hexanes and ethyl acetate in a 15:1 ratio as eluent to give compound **21** (0.28 g, 36%) as a pale yellow solid: mp 277.2 °C (EtOH); ^{1}H NMR (400.13 MHz, DMSO-d_6) δ 11.27 (s, 1H, H1), 8.60 (s, 1H, H8), 8.12 (m, 2H, H*o*), 7.58 (m, 3H, H*m*, H*p*), 3.74 (s, 2H, H3); ^{13}C NMR (100.62 MHz, DMSO-d_6) δ 166.1 (C2), 161.1 (C4), 147.1 (C8), 142.4 (C6), 140.6 (C9a), 136.1 (C*i*), 133.2 (C5a), 132.1 (C*p*), 128.9 (C*m*), 128.1 (C*o*), 115.3 (C7), 40.9 (C3); ^{15}N NMR (40.54 MHz, DMSO-d_6) δ −230.9 (N1), n.o. (N5), −86.7 (N9); anal. calcd for $C_{14}H_9BrClN_3O$ (350.60): C, 47.96; H, 2.59; N, 11.99. Found: C, 47.44; H, 2.64; N, 11.69.

8-Bromo-9-methyl-2-phenyl-3,5-dihydro-4H-pyrido[2,3-b][1,4]diazepin-4-one (22). 5-Bromo-4-methyl-2,3-diaminopyridine (0.50 g, 2.48 mmol) and ethyl benzoylacetate (0.44 mL, 2.55 mmol) in anhydrous xylene (8 mL) were heated at 150 °C for 48 h. Purified by column chromatography using hexanes and ethyl acetate in a 15:1 ratio as eluent to give compound **22** (0.29 g, 35%) as a pale yellow solid: mp 290.4 °C (EtOH); ^{1}H NMR (400.13 MHz, DMSO-d_6) δ 10.98 (s, 1H, H1), 8.44 (s, 1H, H8), 8.11 (dd, $^3J_{Hm}$ = 8.0, $^4J_{Hp}$ = 1.5 Hz, 2H, H*o*), 7.57 (m, 3H, H*m*, H*p*), 3.62 (s, 2H, H3), 2.53 (s, 3H, Me); ^{13}C NMR (100.62 MHz, DMSO-d_6) δ 166.3 (C2), 159.3 (C4), 146.4 (C8), 144.4 (C6), 141.4 (C9a), 136.6 (C*i*), 134.4 (C5a), 131.6 (C*p*), 128.9 (C*m*), 127.8 (C*o*), 117.5 (C7), 40.5 (C3), 16.1 (Me); ^{15}N NMR (40.54 MHz, DMSO-d_6) δ −232.0 (N1), n.o. (N5), −87.6 (N9); anal. calcd for $C_{15}H_{12}BrN_3O$ (330.19): C, 54.56; H, 3.66; N, 12.73. Found: C, 54.50; H, 3.71; N, 12.77.

5-Methyl-2-phenyl-3,5-dihydro-4H-pyrido[2,3-b][1,4]-diazepin-4-one (23). Iodomethane (0.062 mL, 1.00 mmol), K_2CO_3 (0.138 g, 1.00 mmol), and a catalytic amount of KI were added to a solution of **17** (0.21 g, 0.89 mmol) in DMF (1.2 mL), and the mixture was heated at 110 °C for 4 h. After cooling, the mixture was treated with cold water and extracted with ethyl acetate (3 × 3 mL). The organic solvent was evaporated to afford compound **23** (0.19 g, 85%) as a pale yellow solid: mp 124.7 °C (EtOH). ^{1}H NMR (400.13 MHz, CDCl$_3$) δ 8.42 (dd, $^3J_{H7}$ = 4.6, $^4J_{H6}$ = 1.8 Hz, 1H, H8), 8.14 (m, 2H, H*o*), 7.82 (dd, $^3J_{H7}$ = 7.9, $^4J_{H8}$ = 1.8 Hz, 1H, H6), 7.51 (m, 3H, H*m*, H*p*), 7.26 (dd, $^3J_{H6}$ = 7.9, $^3J_{H8}$ = 4.6 Hz, 1H, H7), 4.12 (vb, 1H, H3), 3.52 (s, 3H, Me), 3.12 (vb, 1H, H3); ^{13}C NMR (100.62 MHz, CDCl$_3$) δ 166.0 (C2), 161.2 (C4), 145.8 (C8), 146.1 (C9a), 136.9 (C*i*), 136.6 (C5a), 136.2 (C6), 131.5 (C*p*), 128.8 (C*m*), 127.9 (C*o*), 120.5 (C7), 40.1 (C3), 33.0 (Me); ^{15}N NMR (40.54 MHz, CDCl$_3$) δ −239.1 (N1), n.o. (N5), −85.8 (N9); anal. calcd for $C_{15}H_{13}N_3O$ (251.29): C, 71.70; H, 5.21; N, 16.72. Found: C, 71.58; H, 5.57; N, 15.75.

8-Fluoro-1-methyl-2-phenyl-3,5-dihydro-4H-pyrido[2,3-b][1,4]diazepin-4-one (24). Iodomethane (0.054 mL, 0.86 mmol), K_2CO_3 (0.13 g, 0.94 mmol), and a catalytic amount of KI were added to a solution of **18** (0.20 g, 0.78 mmol) in DMF (1.2 mL) and the mixture was heated at 110 °C for 3 h. After cooling, the mixture was treated with cold water and extracted with ethyl acetate (3 × 3 mL). The organic solvent was evaporated to afford compound **24** (0.17 g, 82%) as a pale yellow solid: mp 144.7 °C (EtOH). ^{1}H NMR (400.13 MHz, CDCl$_3$) δ 8.28 (d, $^4J_{H6}$ = 2.8 Hz, 1H, H8), 8.14 (m, 2H, H*o*), 7.52 (m, 4H, H6, H*m*, H*p*), 4.21 (vb, 1H, H3), 3.34 (s, 3H, Me), 3.04 (vb, 1H, H3); ^{13}C NMR (100.62 MHz, CDCl$_3$) δ 165.6 (C2), 156.2 (C7), 152.2 (C4), 142.5 (C9a), 137.3 (C5a), 136.6 (C*i*), 133.9 (C8), 131.9 (C*p*), 128.9 (C*m*), 128.8 (C*o*), 121.9 (C6), 40.2 (C3), 33.2 (Me); ^{15}N NMR (40.54 MHz, CDCl$_3$) δ n.o. (N1), n.o. (N5), −79.2 (N9); ^{19}F NMR (376.50 MHz, DMSO-d_6) δ −132.0 (d, $^3J_{H6}$ = 8.5 Hz, 1F, F7); anal. calcd for
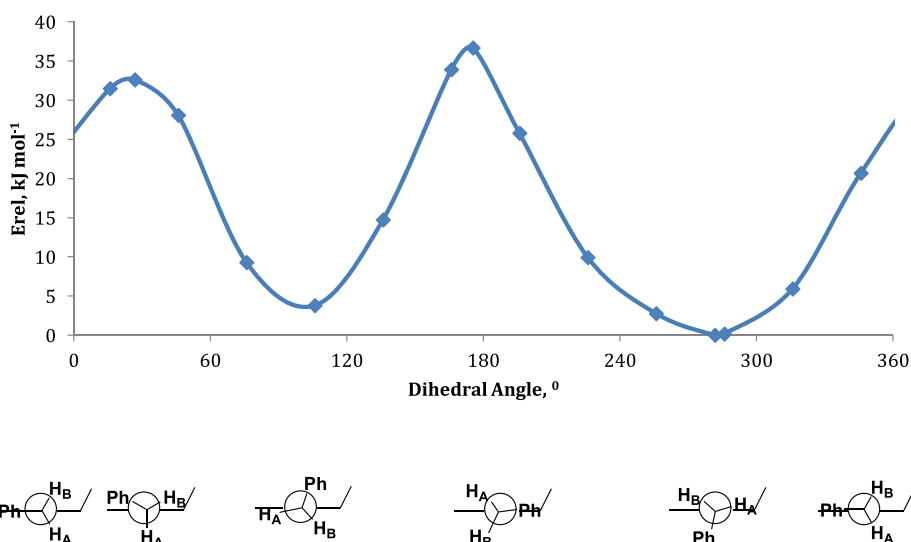
Figure 13. Rotation profile of compound **25** together with Newman projections.

Table 4. Comparison of Experimental and Calculated Chemical Shifts for the Two Rotamers of Compound 25

minimum	nuclei	no. of points	intercept	slope	R^2
first minimum	all	30	+0.0690	0.9997	0.99973
second minimum	all	30	−0.1048	1.0030	0.99956
first minimum	only ^{13}C	17	+0.1954	0.9986	0.99782
second minimum	only ^{13}C	17	−4.2266	1.0343	0.99771

$C_{15}H_{12}FN_3O$ (269.28): C, 66.91; H, 4.49; N, 15.60. Found: C, 65.60; H, 4.49; N, 15.36.

5-Benzyl-2-phenyl-3,5-dihydro-4H-pyrido[2,3-b][1,4]-diazepin-4-one (**25**). Benzyl chloride (0.13 mL, 1.16 mmol), K_2CO_3 (0.175 g, 1.26 mmol), and a catalytic amount of KI were added to a solution of **17** (0.25 g, 1.05 mmol) in DMF (2.5 mL) and the mixture was heated at 110 °C for 5 h. After cooling, the mixture was treated with cold water and extracted with ethyl acetate (3 × 3 mL). The organic solvent was evaporated to afford compound **25** (0.28 g, 80%) as a pale yellow solid: mp 140−142 °C (EtOH); ^{1}H NMR (400.13 MHz, CDCl$_3$) δ 8.39 (dd, $^3J_{H7}$ = 4.6, $^4J_{H6}$ = 1.8 Hz, 1H, H8), 8.14 (m, 2H, Ho), 7.79 (dd, $^3J_{H7}$ = 7.9, $^4J_{H8}$ = 1.8 Hz, 1H, H6), 7.52 (m, 3H, Hm, Hp), 7.22 (dd, $^3J_{H6}$ = 7.9, $^3J_{H8}$ = 4.6 Hz, 1H, H7), 7.13 (m, 5H, Ho-Bn, Hm-Bn, Hp-Bn), 4.30 (vb, 1H, H3), 5.46 (s, 2H, CH$_2$-Bn), 3.07 (vb, 1H, H3); ^{13}C NMR (100.62 MHz, CDCl$_3$) δ 165.1 (C2), 161.4 (C4), 145.8 (C8), 144.9 (C9a), 137.7 (Ci-Bn), 137.2 (Ci), 137.0 (C5a), 136.3 (C6), 126.9 (Cp, Cp-Bn), 128.8 (Cm-Bn), 128.3 (Cm), 127.9 (Co), 127.4 (Co-Bn), 120.7 (C7), 40.3 (C3-Bn), 48.0 (CH$_2$); ^{15}N NMR (40.54 MHz, CDCl$_3$) δ n.o.

(N1), n.o. (N5), −83.6 (N9); anal. calcd for $C_{21}H_{17}N_3O$ (327.39): C, 77.04; H, 5.23; N, 12.84. Found: C, 76.99; H, 5.31; N, 13.00.

N-(3-Aminopyridin-2-yl)-3-phenyl-3-oxopropanamide (**26**, *Enol Form*). 2,3-Diaminopyridine (0.15 g, 1.39 mmol) and ethyl benzoylacetate (0.25 mL, 1.45 mmol) in anhydrous xylene (8 mL) were heated at 120 °C for 6 h. The mixture was cooled down and a solid precipitated. This residue was washed with ethyl ether to give compound **26** (0.07 g, 19%) as a brown solid: mp 159.4 °C (EtOH); ^{1}H NMR (400.13 MHz, DMSO-d_6) δ 9.39 (s, 1H, NH), 8.01 (d, $^3J_{Hm}$ = 7.7, 2H, Ho), 7.80 (dd, $^3J_{H5}$ = 4.7, $^4J_{H6}$ = 1.7, 1H, H6), 7.67 (t, $^3J_{Ho}$ = 7.4, 1H, Hp), 7.57 (m, 2H, Hm), 7.48 (m, 1H, H4), 6.55 (m, 1H, H5), 5.81 (s, 2H, NH$_2$), 4.16 (s, 1H, H8); ^{13}C NMR (100.62 MHz, DMSO-d_6) δ 195.1 (C9), 166.0 (C7), 153.7 (C2), 144.6 (C6), 136.2 (Ci), 133.7 (Cp), 132.0 (C4), 128.8 (Cm), 128.3 (Co), 118.0 (C3), 112.1 (C5), 47.4 (C8); ^{15}N NMR (40.54 MHz, DMSO-d_6) δ −310.7 (NH$_2$), −256.21 (NH), n.o. (N1); anal. calcd for $C_{14}H_{13}N_3O_2$ (255.28): C, 65.87; H, 5.13; N, 16.46. Found: C, 65.28; H, 5.09; N, 16.50.

N-(3-Amino-5-bromo-4-methylpyridin-2-yl)-3-phenyl-3-oxopropanamide (**27**, *Enol Form*). 5-Bromo-4-methyl-2,3-diaminopyridine (0.50 g, 2.48 mmol) and ethyl benzoylacetate (0.44 mL, 2.55 mmol) in anhydrous xylene (8 mL) were heated at 120 °C for 24 h. The mixture was cooled down and a solid precipitated. This residue was washed with ethyl ether to give compound **27** (0.73 g, 85%) as a pale yellow solid: ^{1}H NMR (400.13 MHz, DMSO-d_6) δ 9.48 (s, 1H, NH), 8.02 (d, $^3J_{Hm}$ = 7.6, 2H, Ho), 7.95 (s, 1H, H6), 7.69 (t, $^3J_{Ho}$ = 7.1, 1H, Hp), 7.57 (m, 2H, Hm), 6.05 (s, 2H, NH$_2$), 4.20 (s, 1H, H8); ^{13}C NMR (100.62 MHz, DMSO-d_6) δ 195.7 (C9), 166.1 (C7), 156.0
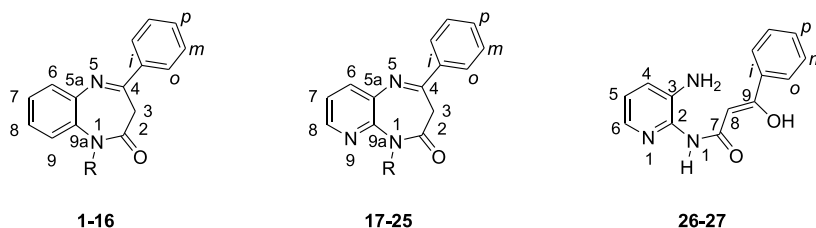

Figure 14. Atom numbering used in the NMR assignments of compounds **1**−**27**.

(C2), 146.6 (C6), 143.8 (C4), 136.1 (C*i*), 133.8 (C*p*), 128.8 (C*m*), 128.3 (C*o*), 117.1 (C3), 108.2 (C5), 47.2 (C8), 17.7 (Me).

Computational Details. The geometries of the molecules were fully optimized with the hybrid HF/DFT B3LYP computational method and the B3LYP/6-311++G(d,p) level.[37,38] Frequency calculations were carried out at the same computational level to verify that the structures obtained correspond to energetic minima (0) or to transition states (TS) (1). These geometries were used for the calculations of the absolute chemical shieldings with the GIAO method.[39,40] All calculations were carried out with the Gaussian-16 package.[41] The following equations were used to transform absolute shieldings into chemical shifts:

$\delta^1 H = 31.0 - 0.97 * \sigma^1 H$ (reference TMS, 0.00 ppm).[42]

$\delta^{13}C = 175.7 - 0.963 * \sigma^{13}C$ (reference TMS, 0.00 ppm).[43]

$\delta^{15}N = -152.0 - 0.946 * \sigma^{15}N$ (reference $MeNO_2$, 0.00 ppm)[43]

$\delta^{19}F = 162.1 - 0.959 * \sigma^{19}F$ (reference $CFCl_3$, 0.00 ppm).[44]

X-ray Crystallography. Data collection for **23** was carried out at 298 K on a Bruker Smart CCD diffractometer using graphite-monochromated Mo-Kα radiation (λ = 0.71073 Å). The system was operated at 50 kV and 35 mA with an exposure time of 20 s in omega. A summary of the fundamental crystal and refinement data is given in Table 5. The structures were solved by direct methods and refined by full-matrix least-squares procedures on F^2 using SHELXS and SHELXL programs, respectively,[45] with the aid of the program Olex2.[46] All nonhydrogen atoms were refined anisotropically. The hydrogen atoms were included in their calculated positions and refined as riding on the respective atoms. CCDC 2003929 contains the supplementary crystallographic data for this paper. These data can be obtained free of charge from The Cambridge Crystallographic Data Centre via https://www.ccdc.cam.ac.uk/structures/.

ASSOCIATED CONTENT

Supporting Information

The Supporting Information is available free of charge at https://pubs.acs.org/doi/10.1021/acsomega.0c03843.

> Calculated, experimental (four solvents), and all (the four solvents together) chemical shifts in ppm (Table S1); ^{1}H NMR chemical shifts and calculation of the inversion barrier of compound **25** (Table S2); electronic energy (Hartree) and Cartesian coordinates (Å) of the structures optimized at the B3LYP/6-311++G(d,p) computational level (Table S3); view of the crystal packing along the *b* axis of **23** (Figure S1); compounds under study ordered differently to make the five different effects appear (Figure S2); ^{1}H, ^{13}C, ^{19}F, and ^{15}N NMR spectra for compounds **17−27** (Figures S3−S66) (PDF)

> Crystallographic data of **23** (CIF)

AUTHOR INFORMATION

Corresponding Author

Marta Pérez-Torralba — *Departamento de Química Orgánica y Bio-Orgánica, Facultad de Ciencias, UNED, E-28040 Madrid, Spain;* orcid.org/0000-0003-0563-8153; Email: mtaperez@ccia.uned.es

Authors

David Núñez Alonso — *Departamento de Química Orgánica y Bio-Orgánica, Facultad de Ciencias, UNED, E-28040 Madrid, Spain*

Rosa M. Claramunt — *Departamento de Química Orgánica y Bio-Orgánica, Facultad de Ciencias, UNED, E-28040 Madrid, Spain;* orcid.org/0000-0001-6634-2677

M. Carmen Torralba — *Departamento de Química Inorgánica, Facultad de Ciencias Químicas, UCM, E-28040 Madrid, Spain*

Patricia Delgado-Martínez — *Unidad de Difracción de Rayos X−CAI Técnicas Físicas y Químicas, Facultad de Ciencias Químicas, UCM, E-28040 Madrid, Spain*

Ibon Alkorta — *Instituto de Química Médica, CSIC, E-28006 Madrid, Spain;* orcid.org/0000-0001-6876-6211

José Elguero — *Instituto de Química Médica, CSIC, E-28006 Madrid, Spain;* orcid.org/0000-0002-9213-6858

Christian Roussel — *Aix-Marseille Univ., CNRS, Centrale Marseille, iSm2, 13397 Marseille, France*

Complete contact information is available at: https://pubs.acs.org/10.1021/acsomega.0c03843

Notes

The authors declare no competing financial interest.

ACKNOWLEDGMENTS

Table 5. Crystal Data and Structure Refinement for 23

crystal data	23
CCDC code	2003929
empirical formula	$C_{15}H_{13}N_3O$
formula weight	251.28
temperature (K)	296.15
crystal system	monoclinic
space group	$C2/c$
a (Å)	21.088(3)
b (Å)	8.6190(13)
c (Å)	17.432(3)
α (°)	90
β (°)	126.527(2)
γ (°)	90
volume (Å^3)	2546.0(7)
Z	8
ρ_{calc} (g/cm^3)	1.311
μ (mm^{-1})	0.085
F(000)	1056.0
2Θ range for data collection (°)	4.808 to 57.61
index ranges	$-28 \leq h \leq 28, -11 \leq k \leq 11, -22 \leq l \leq 22$
reflections collected	12,819
independent reflections [R(int)]	3127 [0.0390]
data/restraints/parameters	3127/0/173
goodness-of-fit on F^2	1.072
R_1 (reflns obsd) $[I \geq 2\sigma(I)]^a$	R_1 = 0.0526 (1858)
wR_2 [all data]^b	wR_2 = 0.1559
largest diff. peak/hole (e Å^{-3})	0.17/−0.20

$^a R_1 = \Sigma||F_o| - |F_c||/\Sigma|F_o|$. $^b wR_2 = \{\Sigma[w(F_o^2 - F_c^2)^2]/\Sigma[w(F_o^2)^2]\}$.

■ REFERENCES

(1) Sankar, R. GABA(A) receptor physiology and its relationship to the mechanism of action of the 1,5-benzodiazepine clobazam. *CNS Drugs* **2012**, *26*, 229−244.

(2) Mendonça Júnior, F. J. B.; Scotti, L.; Ishiki, H.; Botelho, S. P. S.; Da Silva, M. S.; Scotti, M. T. Benzo- and thienobenzo-diazepines: Multi-target drugs for CNS disorders. *Mini-Rev. Med. Chem.* **2015**, *15*, 630−647.

(3) Heinisch, G.; Huber, E.; Leitner, C.; Matuszczak, B.; Maurer, A.; Pachler, S.; Prillinger, U. Pyridazino[3,4-*b*][l,5]benzodiazepin-5-ones: Synthesis and biological evaluation. *Antiviral Chem. Chemother.* **1997**, *8*, 371−379.

(4) Burke, E. W. D.; Morris, G. A.; Vincent, M. A.; Hillier, I. H.; Clayden, J. Is nevirapine atropisomeric? Experimental and computational evidence for rapid conformational inversion. *Org. Biomol. Chem.* **2012**, *10*, 716−719.

(5) Claramunt, R. M.; Alkorta, I.; Elguero, J. A theoretical study of the conformation and dynamic properties of 1,5-benzodiazepines and their derivatives. *Comput. Theor. Chem.* **2013**, *1019*, 108−115.

(6) Pérez-Torralba, M.; Claramunt, R. M.; García, M. A.; López, C.; Torralba, M. C.; Torres, M. R.; Alkorta, I.; Elguero, J. Structure of 1,5-benzodiazepinones in the solid state and in solution: Effect of the fluorination in the six-membered ring. *Beilstein J. Org. Chem.* **2013**, *9*, 2156−2167.

(7) Martín, O.; Pérez-Torralba, M.; García, M. Á.; Claramunt, R. M.; Torralba, M. C.; Torres, M. R.; Alkorta, I.; Elguero, J. Static and dynamic properties of fluorinated 4-aryl-1,5-benzodiazepinones. *ChemistrySelect* **2016**, *1*, 861−870.

(8) Abdel-Ghany, H.; E1-Sayed, A. M.; Sultan, A. A.; E1-Shafei, A. K. A novel syntheses of pyrano[2,3-*c*][1,5]benzodiazepines. *Synth. Commun.* **1990**, *20*, 893−900.

(9) Chniti, S.; Nsira, A.; Khouaja, S.; Mechria, A.; Gharbi, R.; Msaddek, M.; Lecouvey, M. Highly diastereoselective synthesis of rigid 3-enamino-1,5-benzodiazepines. *ARKIVOC* **2018**, *2018*, 283−295.

(10) Mansour, H.; El-Hendawy, M. M. Mechanistic perspectives on piperidine-catalyzed synthesis of 1,5-benzodiazepin-2-ones. *Mol. Catal.* **2020**, *484*, 110774.

(11) Gaponov, A. A.; Anishchenko, A. A. Chemical properties of 2,3-dihydro-1*H*-1,5-benzodiazepinone-2 derivatives: A review. *J. Chem. Technol.* **2013**, *21*, 59−78.

(12) Mtiraoui, H.; Renault, K.; Sanselme, M.; Msaddek, M.; Renard, P. Y.; Sabot, C. Metal-free oxidative ring contraction of benzodiazepinones: An entry to quinoxalinones. *Org. Biomol. Chem.* **2017**, *15*, 3060−3068.

(13) Woltering, T. J.; Wichmann, J.; Goetschi, E.; Knoflach, F.; Ballard, T. M.; Huwyler, J.; Gatti, S. Synthesis and characterization of 1,3-dihydro-benzo[*b*][1,4]diazepin-2-one derivatives: Part 4. In vivo active potent and selective non-competitive metabotropic glutamate receptor 2/3 antagonists. *Bioorg. Med. Chem. Lett.* **2010**, *20*, 6969−6974.

(14) Mtiraoui, H.; Gharbi, R.; Msaddek, M.; Bretonniére, Y.; Andraud, C.; Sabot, C.; Renard, P. Y. 1,5-Benzodiazepin-2-ones: Investigation of a family of photoluminescent materials. *J. Org. Chem.* **2016**, *81*, 4720−4727.

(15) Meanwell, N. A.; Sit, S. Y.; Gao, J.; Wong, H. S.; Gao, Q.; Laurent, D. R. S.; Balasubramanian, N. Regiospecific functionalization of 1,3-dihydro-2*H*-benzimidazol-2-one and structurally related cyclic urea derivatives. *J. Org. Chem.* **1995**, *60*, 1565−1582.

(16) Israel, M.; Jones, L. C.; Modest, E. J. Synthesis and tautomeric behavior of dihydropyrido[2,3-*b*] [1,4]diazepinones. *J. Heterocycl. Chem.* **1967**, *4*, 659−661.

(17) Israel, M.; Jones, L. C. On the reactions of *β*-ketoesters with 2,3-diaminopyridine and its derivatives. *J. Heterocycl. Chem.* **1973**, *10*, 201−207.

(18) Barchet, V. R.; Merz, K. W. Uber kondensationen von nicotinoylessigester mit aromatischen diaminen. *Tetrahedron Lett.* **1964**, *5*, 2239−2244.

(19) Israel, M.; Jones, L. C. Application of a thermal rearrangement Reaction to questions of structure of condensed dihydrodiazepinones: The reaction of 2,3-diaminopyridine with ethyl benzoylacetate. *J. Heterocycl. Chem.* **1969**, *6*, 735−738.

(20) Bonacorso, H. G.; Lourega, R. V.; Deon, E. D.; Zanatta, N.; Martins, M. A. The First synthesis of dihydro-3*H*-pyrido[2,3-*b*][1,4]diazepinols and a new alternative approach for diazepinone analogues. *Tetrahedron Lett.* **2007**, *48*, 4835−4838.

(21) Bonacorso, H. G.; Lourega, R. V.; Porte, L. M.; Deon, E. D.; Zanatta, N.; Flores, A. F.; Martins, M. A. Regiospecific Synthesis of 3*H*-pyrido[2,3-*b*][1,4]diazepin-4(5*H*)-ones via haloform reaction with the isolation of N^3-[3-oxo-4,4,4-trichloroalk-1-en-1-yl]-2,3-diaminopyridine intermediates. *J. Heterocyclc. Chem.* **2009**, *46*, 603−609.

(22) Claramunt, R. M.; López, C.; García, M. A.; Otero, M. D.; Torres, M. R.; Pinilla, E.; Alarcón, S. H.; Alkorta, I.; Elguero, J. The structure of halogeno-1,2,4-triazoles in the solid state and in solution. *New J. Chem.* **2001**, *25*, 1061−1068.

(23) Radula-Janik, K.; Kupka, T.; Ejsmont, K.; Daszkiewicz, Z.; Sauer, S. P. A. Halogen effect on structure and ^{13}C NMR chemical shift of 3,6-disubstituted-*N*-alkyl-carbazoles. *Magn. Reson. Chem.* **2013**, *51*, 630−635.

(24) Alkorta, I.; Elguero, J.; Yáñez, M.; Mó, O.; Montero-Campillo, M. M. Relativistic Effects on NMR Parameters of Halogen-Bonded Complexes. *Molecules* **2019**, *24*, 4399−4413.

(25) Alkorta, I.; Elguero, J.; Rasika Dias, H. V.; Parasar, D.; Martín-Pastor, M. An experimental and computational NMR study of organometallic nine-membered rings: Trinuclear silver(I) complexes of pyrazolate ligands. *Magn. Reson. Chem.* **2020**, *58*, 319−328.

(26) Anet, F. A. L. Ring inversion in cycloheptatriene. *J. Am. Chem. Soc.* **1964**, *86*, 458−460.

(27) Mannschreck, A.; Rissmann, G.; Vögtle, F.; Wild, D. Protonenresonanz-Untersuchungen an siebengliedrigen Ringverbindungen. I. Intramolekulare Beweglichkeit von Azepinen und Diazepinen. *Chem. Ber.* **1967**, *100*, 335−346.

(28) Benassi, R.; Lazzeretti, P.; Taddei, F.; Nardi, D.; Tajana, A. Variable temperature NMR behaviour of 1,5-benzodiazepinones and 1,5-benzodiazepinthiones. *Org. Magn. Reson.* **1976**, *8*, 387−388.

(29) Lewis, G. A.; Mathieu, D.; Phan-Tan-Luu, R. *Pharmaceutical Experimental Design*, Marcel Dekker, New York, 1999.

(30) Carlson, R.; Carlson, J. E. *Design and Optimization in Organic Synthesis*: 2nd Revised Edition, Elsevier, Amsterdam, 2005.

(31) Vanthuyne, N.; Andreoli, F.; Fernandez, S.; Roman, M.; Roussel, C. Synthesis, chiral separation, barrier to rotation and absolute configuration of *N*-(*O*-functionalized-aryl)-4-alkyl-thiazolin-2-one and thiazolin-2-thione atropoisomers. *Lett. Org. Chem.* **2005**, *2*, 433−443.

(32) Belot, V.; Farran, D.; Jean, M.; Albalat, M.; Vanthuyne, N.; Roussel, C. Steric Scale of Common Substituents from Rotational Barriers of *N*-(*o*-Substituted aryl)thiazoline-2-thione Atropisomers. *J. Org. Chem.* **2017**, *82*, 10188−10200.

(33) Iida, A.; Matsuoka, M.; Hasegawa, H.; Vanthuyne, N.; Farran, D.; Roussel, C.; Kitagawa, O. N-C Axially Chiral Compounds with an ortho-Fluoro Substituent and Steric Discrimination between Hydrogen and Fluorine Atoms Based on a Diastereoselective Model Reaction. *J. Org. Chem.* **2019**, *84*, 3169−3175.

(34) Iwasaki, Y.; Morisawa, R.; Yokojima, S.; Hasegawa, H.; Roussel, C.; Vanthuyne, N.; Caytan, E.; Kitagawa, O. N-C Axially Chiral Anilines: Electronic Effect on Barrier to Rotation and A Remote Proton Brake. *Chem. − Eur. J.* **2018**, *24*, 4453−4458.

(35) Furukawa, G.; Shirai, T.; Homma, Y.; Caytan, E.; Vanthuyne, N.; Farran, D.; Roussel, C.; Kitagawa, O. Relayed Proton Brake in *N*-Pyridyl-2-iso-propylaniline Derivative: Two Brakes with One Proton. *J. Org. Chem.* **2020**, *85*, 5109−5113.

(36) Braun, S.; Kalinowski, H.-O.; Berger, S. *150 and More Basic NMR Experiments*; Wiley VCH: New York, 1998.

(37) Ditchfield, R. H. W. J.; Hehre, W. J.; Pople, J. A. Self-Consistent Molecular Orbital Methods. IX. An Extended Gaussian-Type Basis for Molecular Orbital Studies of Organic Molecules. *J. Chem. Phys.* **1971**, *54*, 724−728.

(38) Frisch, M. J.; Pople, J. A.; Binkley, J. S. Self-Consistent Molecular Orbital Methods. 25. Supplementary Functions for Gaussian Basis Sets. *J. Chem. Phys.* **1984**, *80*, 3265−3269.

(39) London, F. Quantum Theory of Interatomic Currents in Aromatic Compounds. *J. Phys. Radium* **1937**, *8*, 397−409.

(40) Ditchfield, R. Self-consistent Perturbation Theory of Diamagnetism. I. A Gauge-Invariant LCAO (Linear Combination of Atomic Orbitals) Method for NMR Chemical Shifts. *Mol. Phys.* **1974**, *27*, 789−807.

(41) Frisch, M. J., Trucks, G. W., Schlegel, H. B., Scuseria, G. E., Robb, M. A., Cheeseman, J. R., Scalmani, G., Barone, V., Petersson, G. A., Nakatsuji, H., Li, X., Caricato, M., Marenich, A. V., Bloino, J., Janesko, B. G., Gomperts, R., Mennucci, B., Hratchian, H. P., Ortiz, J. V., Izmaylov, A. F., Sonnenberg, J. L., Williams-Young, D., Ding, F., Lipparini, F., Egidi, F., Goings, J., Peng, B., Petrone, A., Henderson, T., Ranasinghe, D., Zakrzewski, V. G., Gao, J., Rega, N., Zheng, G., Liang, W., Hada, M., Ehara, M., Toyota, K., Fukuda, R., Hasegawa, J., Ishida, M., Nakajima, T., Honda, Y., Kitao, O., Nakai, H., Vreven, T., Throssell, K., Montgomery, Jr., J. A., Peralta, J. E., Ogliaro, F., Bearpark, M. J., Heyd, J. J., Brothers, E. N., Kudin, K. N., Staroverov, V. N., Keith, T. A., Kobayashi, R., Normand, J., Raghavachari, K., Rendell, A. P., Burant, J. C., Iyengar, S. S., Tomasi, J., Cossi, M., Millam, J. M., Klene, M., Adamo, C., Cammi, R., Ochterski, J. W., Martin, R. L., Morokuma, K., Farkas, O., Foresman, J. B., Fox, D. J. Gaussian 16, Revision A.03, Gaussian, Inc., Wallingford CT 2016.

(42) Silva, A. M. S.; Sousa, R. M. S.; Jimeno, M. L.; Blanco, F.; Alkorta, I.; Elguero, J. Experimental measurements and theoretical calculations of the chemical shifts and coupling constants of three azines (benzalazine, acetophenoneazine and cinnamaldazine). *Magn. Reson. Chem.* **2008**, *46*, 859−864.

(43) Blanco, F.; Alkorta, I.; Elguero, J. Statistical analysis of ^{13}C and ^{15}N NMR chemical shifts from GIAO/B3LYP/6-311++G** calculated absolute shieldings. *Magn. Reson. Chem.* **2007**, *45*, 797−800.

(44) Fresno, N.; Pérez-Fernández, R.; Jimeno, M. L.; Alkorta, I.; Sánchez-Sanz, G.; Elguero, J.; Del Bene, J. E. Multinuclear NMR characterization of cyanuric fluoride (2,4,6-trifluoro-1,3,5-triazine). *J. Heterocycl. Chem.* **2012**, *49*, 1257−1259.

(45) (a) Sheldrick, G. M. Crystal structure refinement with SHELXL. *Acta Crystallogr., Sect. C: Struct. Chem.* **2015**, *71*, 112−118. (b) Sheldrick, G. M. SHELXT - Integrated space-group and crystal-structure determination. *Acta Crystallogr., Sect. A: Found. Adv.* **2015**, *71*, 3−8.

(46) Dolomanov, O. V.; Bourhis, L. J.; Gildea, R. J.; Howard, J. A. K.; Puschmann, H. OLEX2: a complete structure solution, refinement and analysis program. *J. Appl. Crystallogr.* **2009**, *42*, 339−341.